MSUCL-231
December 1976

The Neutron Time-of-Flight Facility at Michigan State University*

Ranjan K. Bhowmik, Robert R. Doering, Lawrence E. Young,
Sam M. Austin, Aaron Galonsky and Steve D. Schery+

Cyclotron Laboratory and Physics Department
Michigan State University, East Lansing, Michigan 48824

Abstract

A new neutron time-of-flight facility at the Michigan State University Cyclotron Laboratory incorporates a magnetic beam swinger permitting measurement of angular distributions with a stationary detector. A large volume (2.7ℓ) liquid scintillation detector with a time resolution of less than 200 ps was developed to exploit the long flight paths (4-32 meters) made possible by the swinger. For 33 MeV neutrons an overall time (energy) resolution of 550 ps (≃ 150 keV) has been achieved.

---

*Supported by the National Science Foundation

+Presently at Moody College, Galveston, Texas

1. INTRODUCTION

A neutron time-of-flight (TOF) facility incorporating a beam swinger[1] has been constructed at the Michigan State University Cyclotron Laboratory. In this arrangement the neutron counter is held fixed; to change the reaction angle, the direction of the beam on target is changed by moveable magnets. Flight paths of 4 to 32 m are possible in a compact experimental area. The beam dump and the detector are housed in separate rooms facilitating good shielding. To have reasonable counting rates for the longer flight paths, a neutron detector with a volume of 2.7 liters of NE224 scintillator has been developed. The analog signals from the detector are digitized and processed in a PDP11/45 computer connected to a CAMAC crate. An overall time resolution of 550 ps has been obtained with roughly equal contributions from beam resolution, target thickness and counter resolution.

2. BEAM SWINGER

The physical layout of the beam swinger is shown in fig. 1. The charged particle beam from the cyclotron is bent 90° by a fixed magnet and enters the swinger along the horizontal axis of rotation. The two swinger magnets bend the beam by -45°, and 135°, respectively, so that the beam, after emerging from the swinger, is perpendicular to the original direction. The 90° magnet provides energy analysis with a dispersion in energy of 7×10^{-4}/mm, and because the beam enters non-radially also contributes focussing strength. Double focuses occur at the entrance to the 90° magnet, near the entrance to the swinger and at the target (points 1,2 and 3 of fig. 1).

The swinger magnets are of the H design with a bending radius of 76 cm. The poles are 10.2 cm wide and have a 3.2 cm gap with a 36 minute taper on each poletip to provide double focussing (n=1/2). The overall magnification of the swinger system is about one, typically resulting in a beam spot 2 mm square on target.

The magnet material used is fully annealed 1010 steel. From estimates of fringing field effects, the physical lengths of the steel were cut to 44° and 134°, and the chamfers at the entrance and exit pole corners were cut 2.5 cm deep. To reduce saturation effects, there is a 45° chamfer all around the pole edges, leaving a width of 7.0 cm at the tip of each pole and the combined thickness of the two arms of the return yoke is 12.7 cm, i.e., 2.5 cm greater than the pole width.

The current carrying coils are flat pancakes, three to each pole, made of 1.2 cm square, hollow-conductor copper wrapped in fiber-glass and vacuum potted in epoxy. Current and power consumption at a field of 1.4 Tesla are 450 A and 22 kW, respectively. This field strength is sufficient to bend 76 MeV $^{3}He^{++}$ ions, our most rigid beam.

For studying (charged particle, n) reactions, the target is placed on the axis of rotation of the swinger, as shown in fig. 2a. The proton beam is stopped in a water-filled Faraday cup. Neutrons from the target emerge in a horizontal plane through an opening in a 1.8 meter thick concrete shielding wall into a long hallway. Flight paths of from 4 to 32 meters may be obtained by moving the detector. By rotating the swinger magnet, the reaction angle may be changed from 0° to 165° beyond which point the magnet yoke blocks the flight path; there is a hole in the yoke so that an angle of 180° is also available. For reaction angles of less than 6°, the beam dump is not

shielded from the detector.

The beam from the MSU Cyclotron is sharply bunched in time, with a typical burst width of ≈ 300 ps and a burst interval between 50 and 67 ns depending upon particle energy. At long flight paths or when a large dynamic range of neutron energy is required, it is necessary to increase the interval between pulses. This is accomplished by an external beam pulser[2] which deflects away the unwanted beam burst using electrostatic beam sweeper plates.

For neutron scattering experiments (see fig. 2b) a neutron beam is generated by protons striking a ^{7}Li target, placed, depending upon angle, 10-26 cm from the axis of rotation. Neutrons from the ^{7}Li(p,n) reaction (Q=-1.644 MeV) bombard cylindrical scattering samples placed on the axis. The proton beam, after passsing thru a 0.05 mm thick aluminium foil, is stopped in a water-filled Faraday cup. Because the Q value of the ^{16}O (p,n) reaction is so negative ($Q \leq -16.2$ MeV), little background is produced in the region of the main ^{7}Li(p,n) peak. It is necessary to shield the detector from the neutron production target and Faraday cup; this is done with a 300 kg iron shadow bar whose position can be adjusted by remote control.

3. NEUTRON DETECTION SYSTEM

3.1 DETECTOR

The present detector is similar in principle to the detector described in ref. 3. By using a rectangular box of ultra-violet-transmitting lucite (PLEXIGLAS G^{+}) of 84 cm x 13 cm x 2.5 cm internal dimensions to contain the liquid scintillator NE224^{++}, a large volume

---

$^{+}$Obtained from Rohm and Haas Company, Philadelphia, PA 19105

$^{++}$Obtained from Nuclear Enterprises, Inc., San Carlos, CA 94070

of scintillator is achieved with a detector which is thin in the direction of incident neutrons. Two detectors consisting of glass cylinders filled with NE213, but otherwise similar to the one detailed here, are described in refs. 4 and 5. Experiments with a prototype detector indicated that when machined surfaces of lucite were glued together with dichloro-methane and exposed to NE224, they developed micro-cracks within a few days. To minimize the number of glued joints exposed to NE224, the main body of the detector was machined from a single slab of PLEXIGLAS G. The open side of this structure was closed by the addition of a 1.0 cm thick lid of the same material. In order to enhance total internal reflection the exterior surfaces of the lucite were left in as-cast condition wherever possible. A small lucite chamber is attached to the box to allow for thermal expansion of the liquid. The light pipes are also made of PLEXIGLAS G and are viewed by two RCA8575 photomultipliers. The anode signals and linear signals from the ninth dynodes are extracted with ORTEC 265 photomultiplier bases. Details of the box and the light pipes are shown in fig. 3. The detector is wrapped with white paper and is made light tight by covering with aluminium foil and black tape.

3.2 ELECTRONICS

A block diagram of the electronics is shown in fig. 4. The times of arrival at the photomultiplier anodes, T_1 and T_2, of the light flashes from a neutron event are extracted using constant fraction discriminators. The time T_1 with respect to the cyclotron RF and the time difference T_2-T_1 are measured by time to amplitude converters (TAC). Because of the difference in optical paths, both T_1 and the time difference T_2-T_1 are dependent on the distance of the light

producing event from the photomultipliers. The average time, $(T_1 + T_2)/2$ is, on the other hand, independent of this location and gives the relative TOF. The counter may also be used as a position sensitive detector, using T_2-T_1 for position information along the length of the counter.

To obtain pulse shape discrimination (PSD) between neutrons and gammas[6], the dynode pulses are amplified and shaped by double-delay-line shaping amplifiers. The rise times (to 0.5 of full amplitude) of the dynode pulses are obtained by starting a TAC with the zero-crossing timing signal for the (double-delay-line shaped) linear pulse and stopping with the (delayed) anode pulse. The total light output (E_1+E_2) from the summing amplifier and the time signals T_1, T_2-T_1, PSD_1 and PSD_2 are fed to a PDP11/45 computer for further processing.

3.3 COMPUTER PROGRAM

The multiparameter data from the neutron detector are digitized in an ORTEC octal 12-bit ADC (AD811) and stored in a data buffer. A FORTRAN program has been written for processing the data, calculating $(T_1+T_2)/2$ and storing up to eight one-dimensional spectra. The TOF spectra can be gated by the total light output in the scintillator and/or by the PSD signal to separate neutron events from gamma-ray events. Two-dimensional displays are available during setup procedures. The conversion time of the ADC limits the data rate to about 2000 events per second.

3.4 DETECTOR PERFORMANCE

The light pulses reaching a photomultiplier due to events in the far end of the detector are attenuated by absorption in the scintillator and in surface irregularities of the sides of the detector. For the

present detector, the attenuation is 46% from one end to the other. As one raises the light threshold the time resolution improves but the neutron detection efficiency decreases. In order to provide several choices during analysis, TOF spectra gated by different light thresholds are simultaneously collected in the computer.

For end-to-end timing, i.e., T_2-T_1, with a collimated neutron beam, time resolutions of 0.75 ns and 0.32 ns FWHM are obtained for light pulses corresponding to 2.4 and 16 MeV of electron energy. These correspond to position resolutions of 6 cm and 2.5 cm FWHM, respectively, along the length of the counter. The contribution to the time resolution measured with respect to the cyclotron radio frequency is half of these values, namely, 0.38 and 0.16 ns FWHM. The time resolution is best in the center 50 cm of the counter, and the quoted numbers correspond to this region. Near the ends of the detector the time resolution deteriorates by about 25%. Another detector, which was 1.25 cm thick and was viewed with RCA 8850 photomultipliers, but with otherwise similar construction, had essentially identical time resolution.

Pulse shape discrimination spectra from one photomultiplier for events generated at different parts of the detector are shown in fig. 5. These spectra were obtained with an Am-Be neutron source using a light threshold of 2.4 MeV electron energy. The PSD separation of neutron events from gamma ray events is best at the near end of the detector. To optimize the separation for the whole detector, the PSD information is taken from either PSD_1 or PSD_2, depending upon the value of T_2-T_1. This "composite" PSD is then used to gate the TOF spectrum.

4. RESULTS

4.1 (p,n) REACTIONS

Using the swinger facility, we have studied (p,n) reactions on several targets at 25, 35 and 45 MeV. Flight paths up to 32 meters have been used. Proton beams typically have an intensity of 1-2 μa on target. A typical time of flight spectrum for the $^{7}Li(p,n)^{7}Be$ reaction is shown in fig. 6. The time of flight resolution for a light threshold of 16 MeV electron energy is 550 ps FWHM, with roughly equal contributions from detector resolution, target thickness and beam burst width. This corresponds to an energy resolution of 150 keV for 33 MeV neutrons at a flight path of 19.18 meters. The various contributions to time resolution are listed in table 1.

4.2 NEUTRON SCATTERING

Because of the low intensities encountered in neutron scattering studies, one must use thick neutron production targets and have the detector relatively close to the scatterer. Consequently, shielding replaces good time resolution as the dominant concern. In the present arrangement, the target and detector are in separate rooms, simplifying the problem. Figure 7a shows a spectrum from $^{27}Al(n,n)^{27}Al$ at E_n=26 MeV. A generally small "target out" background has been subtracted. The spectrum is rather clean; most of the counts below the main elastic scattering peak reflect the structure in the TOF spectrum of primary neutrons from the $^{7}Li(p,n)^{7}Be$ reaction at 0° (fig. 7b). The energy width of the primary neutron beam is approximately 1 MeV FWHM, arising mainly from the target thickness and the 25% intensity of the 429 keV level in ^{7}Be.

5. SUMMARY

A neutron time of flight system incorporating a beam swinger and a stationary large volume neutron detector has been put into operation. The neutron detector has an intrinsic resolution better than 200 ps for events depositing more than 16 MeV electron energy in the scintillator. This, combined with the narrow time structure of the cyclotron beam, results in an overall resolution of 550 ps in the TOF spectrum. Good shielding and the convenience of a large volume fixed detector at a long flight path make the swinger ideal for high resolution neutron spectroscopy.

It is a pleasure to acknowledge the contributions of H.G. Blosser and G. Stork in the design of the swinger and of R. DeVito and S. Francis in data taking. The assistance of R. Au, C. Morgan and other members of the technical staff of the Cyclotron Laboratory is appreciated.

References

1. D.A. Lind, R.F. Bentley, J.D. Carlson, S.D. Schery, and C.D. Zafiratos, Nucl. Instr. and Meth. 130(1975)93.
C.D. Goodman, M.B. Greenfield, C.A. Goulding and C.C. Foster, BAPS 21(1976)1007.

2. P. Miller and P. Marchand, Michigan State Univ., Private communication.

3. G. Charpak, L. Dick, and L. Feuvais, Nucl. Instr. and Meth. 15(1962)318.

4. V. Giordano, C. Manduchi, M.T. Russo-Manduchi, and G.F. Segato, Nucl. Instr. and Meth. 135(1976)483.

5. D. Evers, E. Spindler, P. Konrad, K. Rudolph, W. Assmann and P. Sperr, Nucl. Instr. and Meth. 124(1975)23.

6. R.B. Owen, I.R.E. Trans. Nucl. Sci. NS-5, No. 3(1958)198.

TABLE 1

Contributions to TOF resolution for 33 MeV neutrons (19.18m flight path)

	time resolution (ps)	energy resolution (keV)
intrinsic time resolution	200	53
detector thickness[a)]	160	43
target thickness	370	100
beam energy spread	110	30
beam time spread	∿300	∿80
total observed	550	150

a) Detector was 1.25 cm thick.

Figure Captions

Fig. 1. Top view of the beam swinger set at a 0° reaction angle. Focusses occur at points 1, 2, and 3, and the target is placed at position 3. The (charged particle,n) chamber is shown in place.

Fig. 2(a). The setup for (charged particle,n) experiments. A NaI detector is used to monitor particles elastically scattered from the target.

(b). Details of the target region for (n,n) experiments.

Fig. 3. Photographs of the detector (filled with scintillator) and light pipe assembly. Lower: Entire detector, direction of incidence of neutrons into the page. Middle: Detail of right hand end of detector. Upper: detail of light pipes.

Fig. 4. Schematic diagram of the electronics. The logic output is used as a strobe to read the five analog signals into a Camac ADC interfaced with a PDP 11/45 computer.

Fig. 5. Pulse Shape Discrimination (PSD) spectra from events occurring at differing distances from the photomultiplier at one end of the detector. The average effects of signal attenuation are reduced in the composite spectrum (see text).

Fig. 6. Time-of-flight spectrum from the $^{7}Li(p,n)^{7}Be$ reaction taken at a flight path of 19.18 meters. The two peaks correspond to the ground state and the 429 keV state in ^{7}Be.

Fig. 7. Time-of-flight spectra taken in the neutron scattering setup with a flight path of 8 meters. A stop pulse is taken from every other RF cycle, resulting in a doubled spectrum. Bottom: spectrum of neutrons from the ^{7}Li production target at 0°. Top: spectrum of neutrons elastically scattered at 20° from a cylindrical aluminum scatterer.

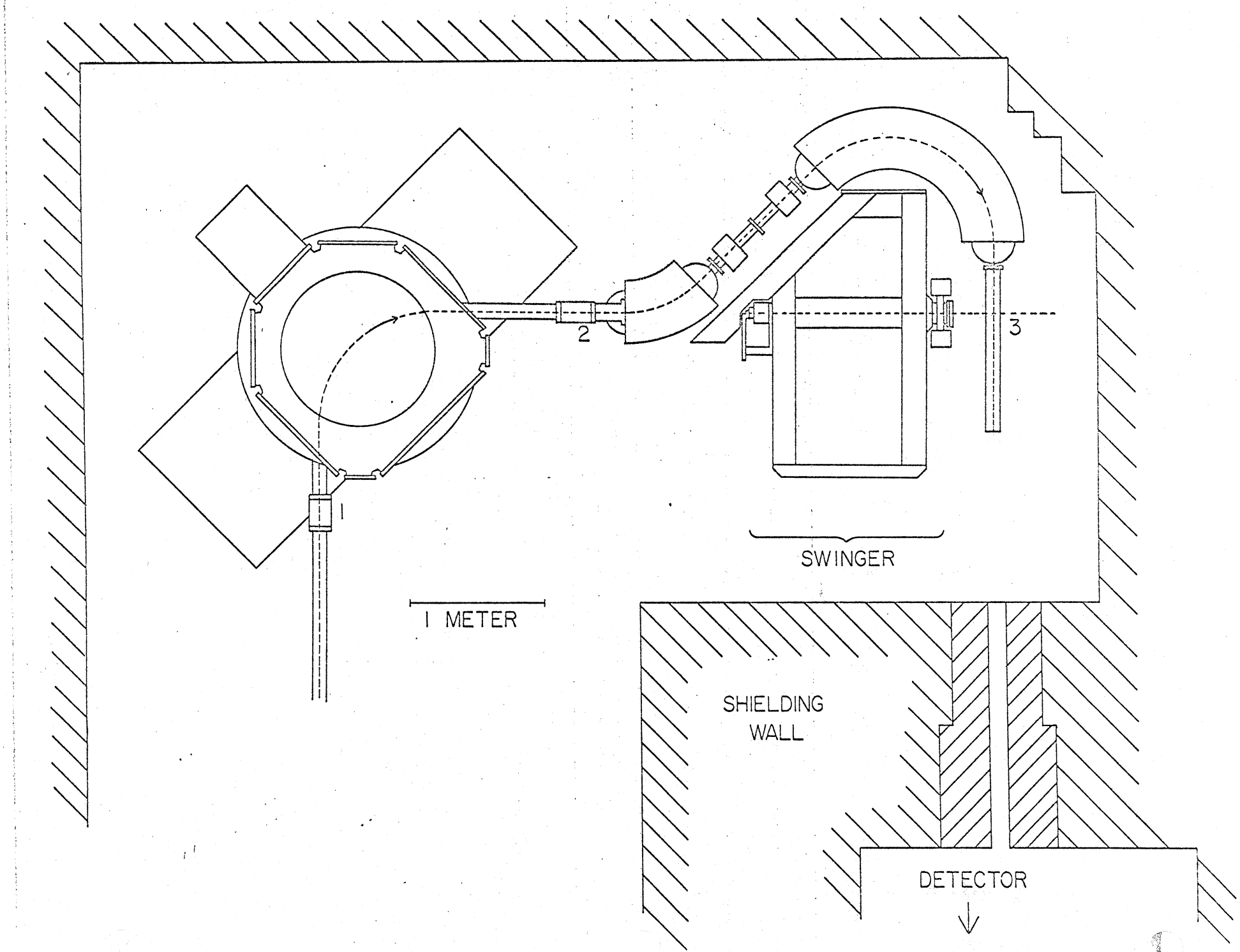
1
2
3
SWINGER
1 METER
SHIELDING
WALL
DETECTOR

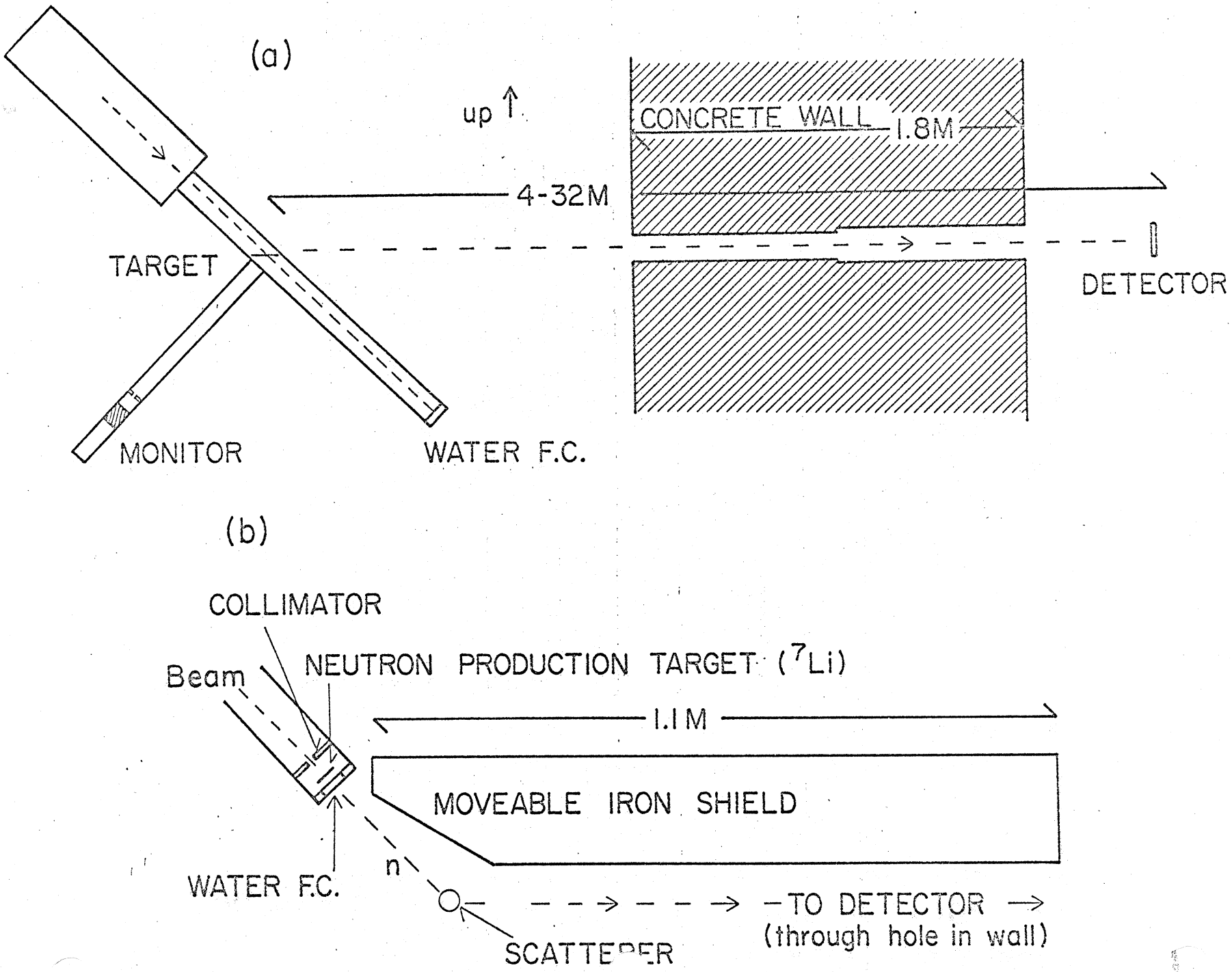
(a)
up
CONCRETE WALL
1.8M
4-32M
TARGET
DETECTOR
MONITOR
WATER F.C.
(b)
COLLIMATOR
Beam
NEUTRON PRODUCTION TARGET (^{7}Li)
1.1 M
MOVEABLE IRON SHIELD
WATER F.C.
n
TO DETECTOR
(through hole in wall)
SCATTERER

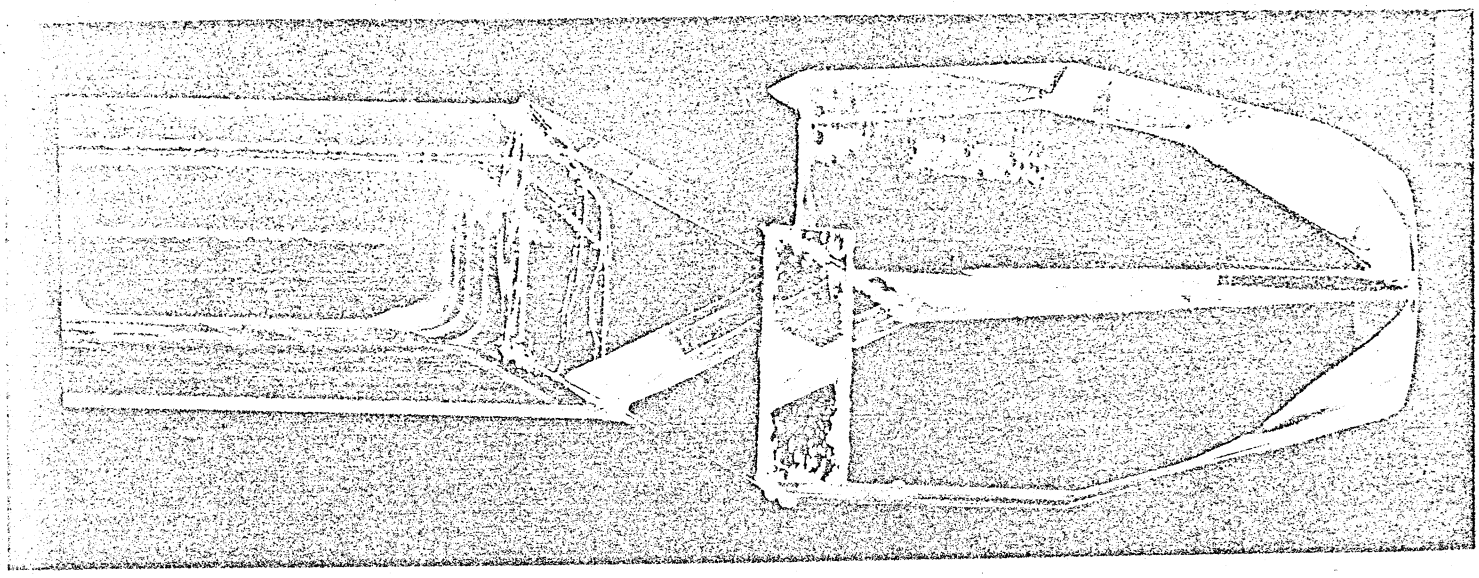

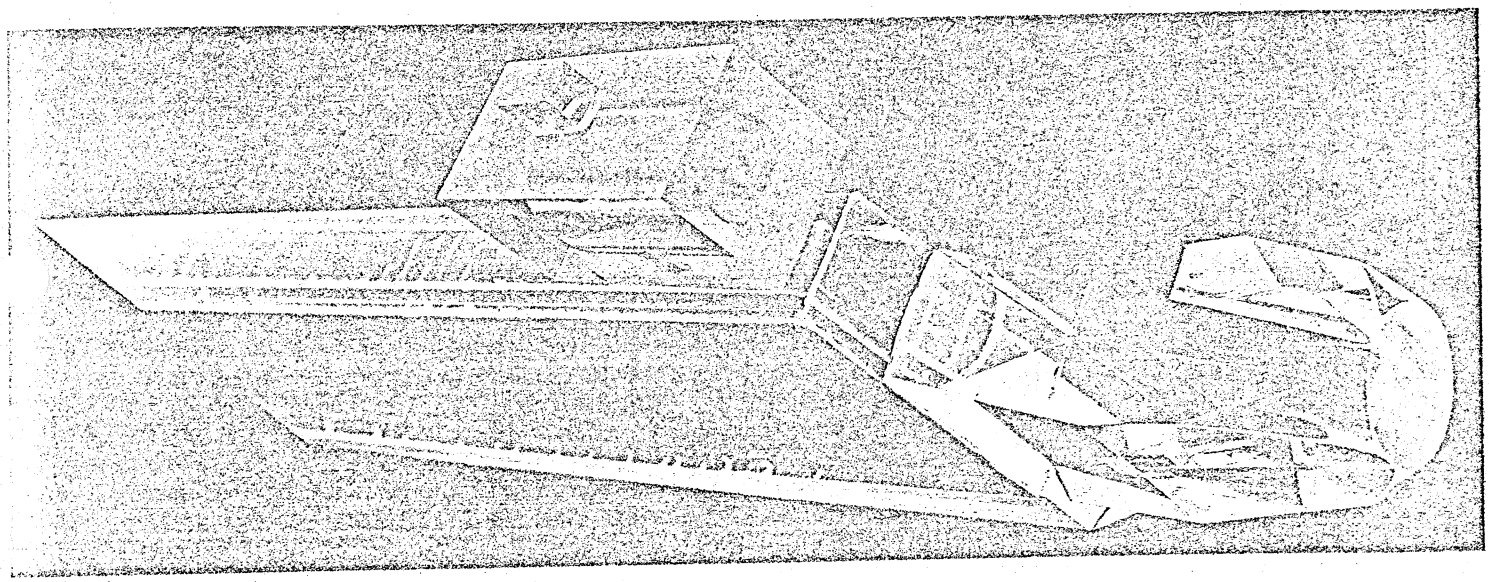

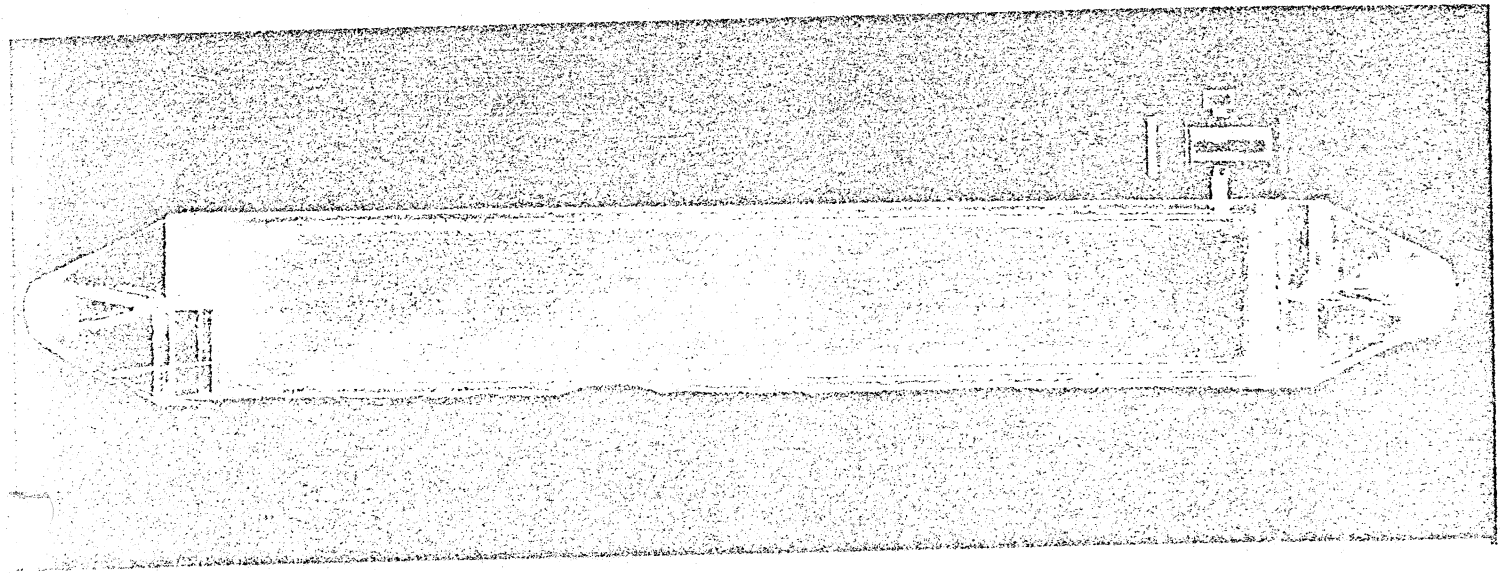

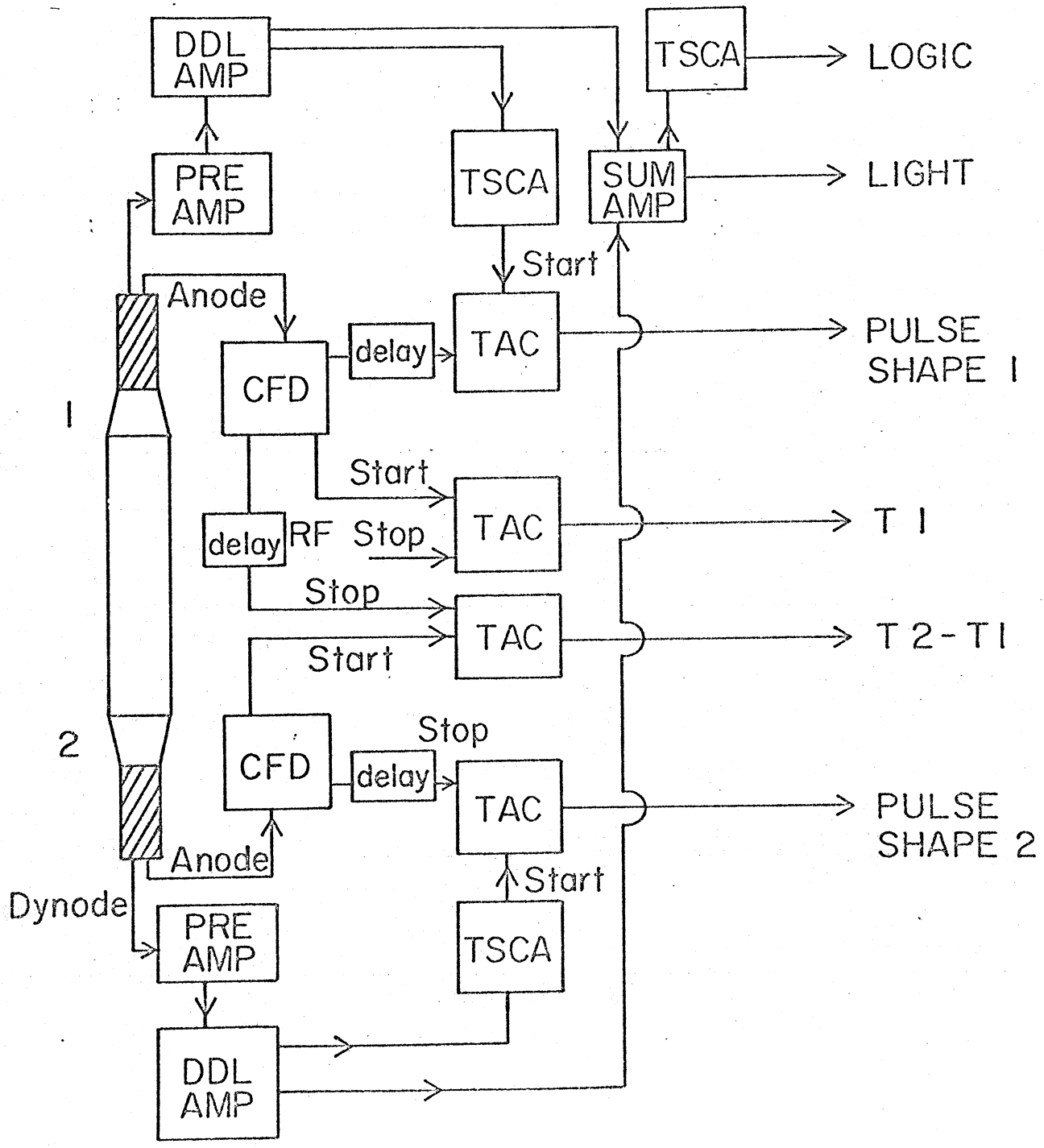

NEUTRON TIME OF FLIGHT ELECTRONICS

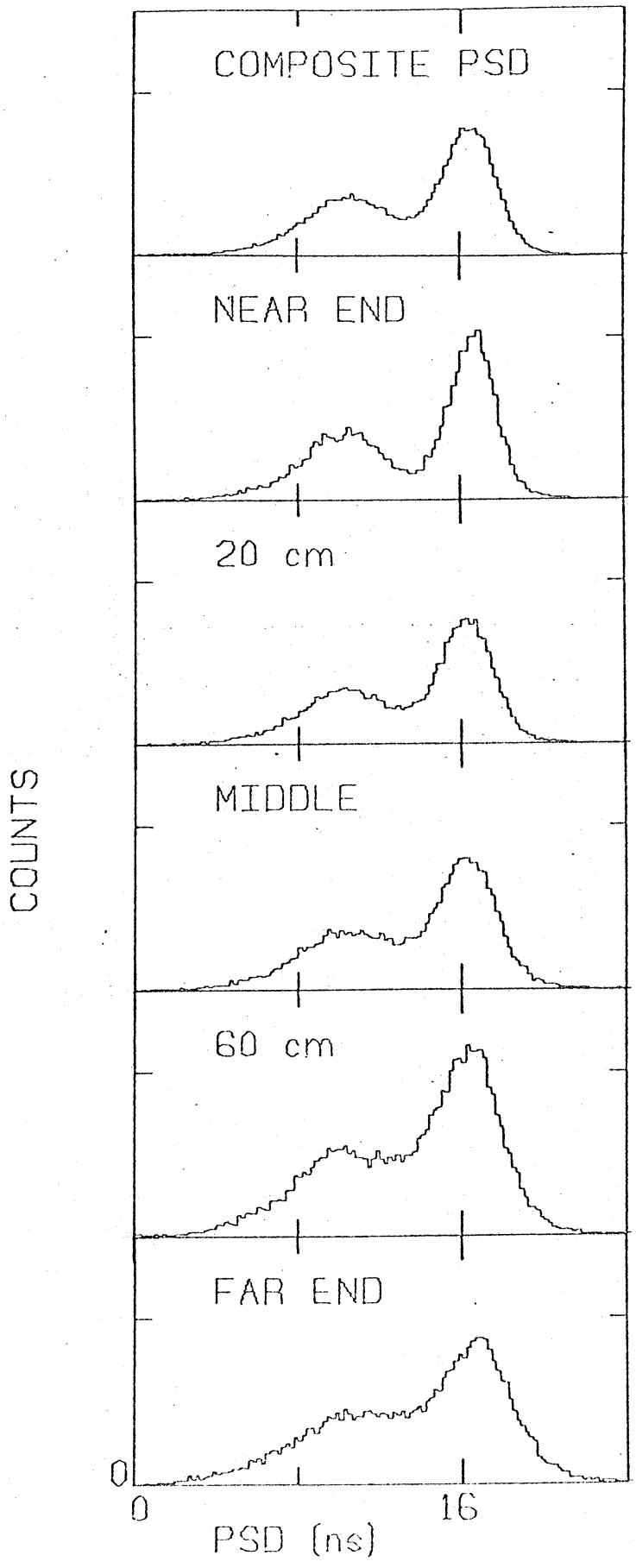
COMPOSITE PSD
NEAR END
20 cm
MIDDLE
60 cm
FAR END
COUNTS
0
0
16
PSD (ns)

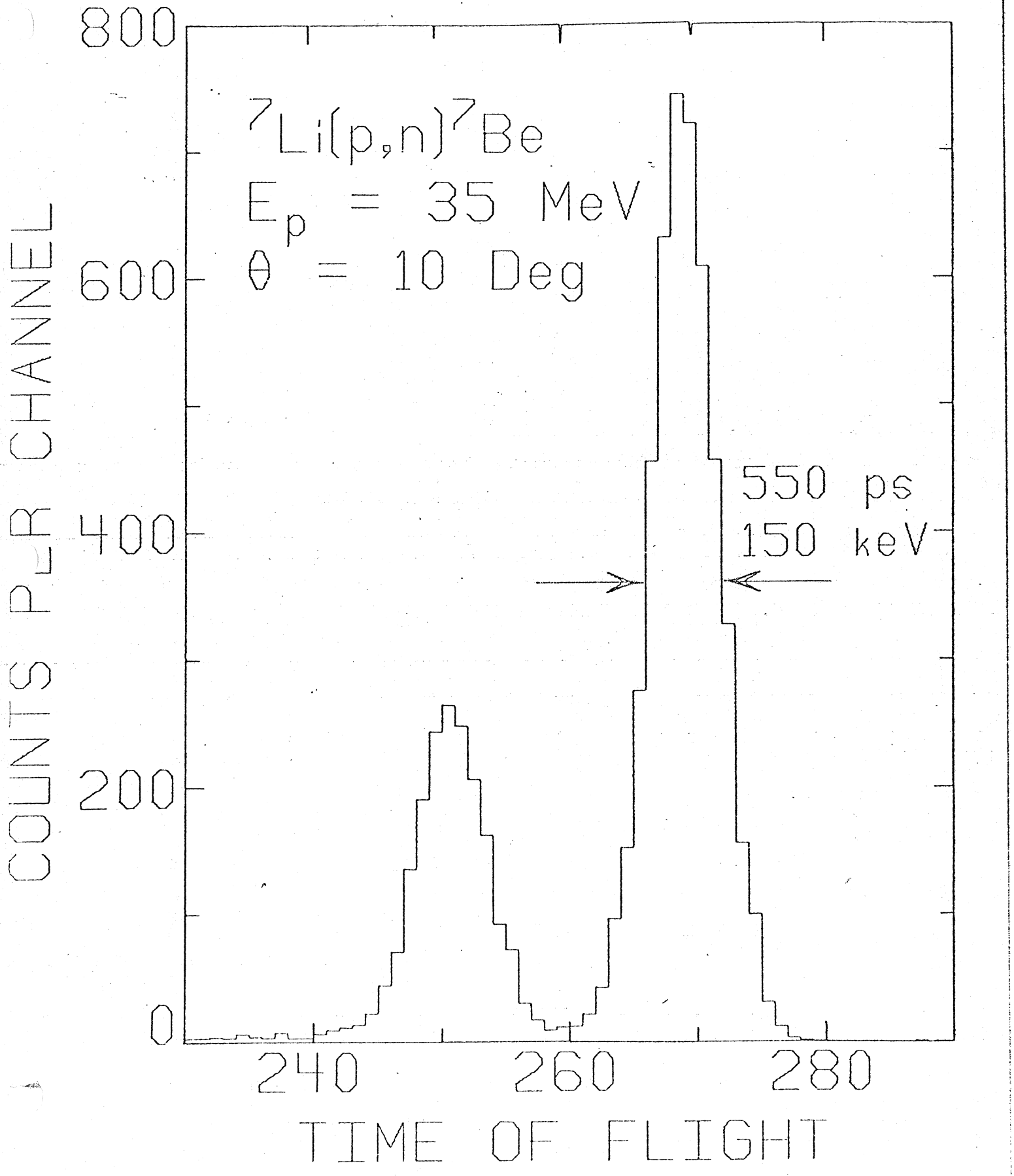
800
600
400
200
0
$^7Li(p,n)^7Be$
E_p = 35 MeV
θ = 10 Deg
550 ps
150 keV
240
260
280
TIME OF FLIGHT
COUNTS PER CHANNEL

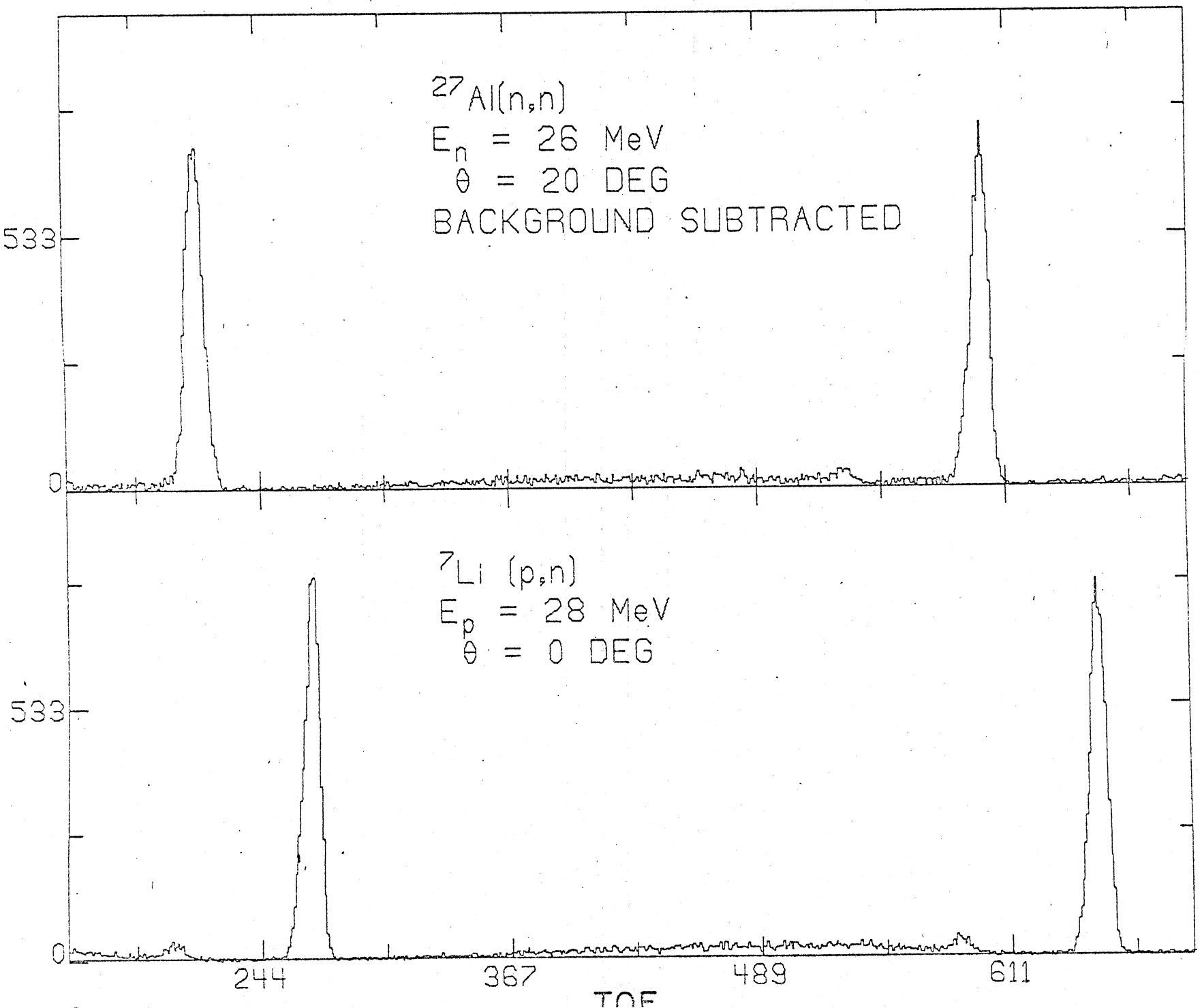
^{27}Al(n,n)
E_n = 26 MeV
θ = 20 DEG
BACKGROUND SUBTRACTED
533
0
^{7}Li (p,n)
E_p = 28 MeV
θ = 0 DEG
533
0
244
367
489
611
TOF